Current Trends in Biotechnology and Pharmacy
Vol. 20 (Supplementary Issue 2A), June 2026, ISSN 0973-8916 (Print)., 2230-7303 (Online)
10.5530/ctbp.2026.2s.14

A Systems Pharmacology Study on Lanifibranor for the Management of Non-Alcoholic Fatty Liver Disease

Ramya Sunkara, and Jithendra Chimakurthy*

Department of Pharmaceutical Sciences, School of Biotechnology and Pharmaceutical Sciences, Vignan's foundation for Science, Technology, and Research, Vadlamudi - 522213, Guntur, Andhra Pradesh, India
*Corresponding author: drjc_pharma@vignan.ac.in

Abstract

Non-alcoholic fatty liver disease (NAFLD) is a prevalent and progressive metabolic liver disorder with limited pharmacological treatment options. Lanifibranor, a pan-peroxisome proliferator-activated receptor (pan-PPAR) agonist, has demonstrated promising therapeutic effects in clinical studies, yet its comprehensive mechanism of action remains unclear. This study employed a systems pharmacology approach integrating network pharmacology, protein–protein interaction (PPI) analysis, functional enrichment, and molecular docking to elucidate the multi-target actions of Lanifibranor in NAFLD. A total of 102 Lanifibranor-associated protein targets and 1,526 NAFLD-related genes were retrieved from public databases, with 37 overlapping targets identified. Network analysis revealed hub genes including PTGS2, MMP9, ESR1, and BCL2 as central regulators in the disease network. Gene Ontology and KEGG enrichment analysis indicated involvement in oxidative stress responses, lipid metabolism, inflammation, and fibrotic signalling pathways showing the involvement of PPAR and AGE–RAGE pathways. Molecular docking confirmed strong binding affinities of Lanifibranor to key targets, particularly PTGS2 (–8.2 kcal/mol) and BCL2 (–8.1 kcal/mol), suggesting anti-inflammatory and anti-apoptotic potential. These findings offer mechanistic insight into Lanifibranor's pleiotropic actions and support its development as a multitargeted therapeutic agent for NAFLD management.

Keywords: Lanifibranor, NAFLD, Systems Pharmacology, PPAR Agonist, Molecular Docking

Introduction

Non-alcoholic fatty liver disease (NAFLD) represents a major global health challenge, with an estimated prevalence of over 25% in the general population and rising sharply in parallel with the obesity and type 2 diabetes epidemics (1). As a complex metabolic liver disorder, NAFLD encompasses a continuum of pathological states ranging from benign steatosis to non-alcoholic steatohepatitis (NASH) (2), progressive fibrosis, cirrhosis, and hepatocellular carcinoma (HCC) (3). The multifactorial nature of NAFLD pathogenesis—driven by lipid accumulation, insulin resistance, oxidative stress, mitochondrial dysfunction, inflammation, and fibrosis—makes it a prototypical systems-level disease (4). Despite the rising burden, there are currently no FDA- or EMA-approved pharmacological treatments for NAFLD or NASH, underscoring the urgent need to identify novel, multitargeted therapeutic agents.

Lanifibranor (IVA337), a pan-peroxisome proliferator-activated receptor (pan-PPAR) agonist, has emerged as a promising therapeutic candidate due to its ability to concurrently activate PPARα, PPARδ, and PPARγ isoforms (5). Through this tri-modal activation, Lanifibranor modulates key metabolic and fibrotic pathways, influencing lipid homeostasis, inflammation, and hepatic stellate cell activation (6). Notably, recent clinical studies have demonstrated Lanifibranor's ability to improve both steatosis and fibrosis in NASH patients, positioning it as a potential disease-modifying agent (7–9). However, given the intricacies of NAFLD pathophysiology, a systems pharmacology-based investigation is

Vol. 20 (Supplementary Issue 2A), June 2026, ISSN 0973-8916 (Print)., 2230-7303 (Online)
10.5530/ctbp.2026.2s.14

imperative to comprehensively understand its multi-target interactions and underlying mechanisms.

Network pharmacology, an emerging discipline rooted in systems biology, offers an integrative framework to elucidate the polypharmacological effects of bioactive compounds by constructing drug–target–pathway–disease networks (10). Unlike reductionist approaches, network pharmacology enables the identification of functionally relevant targets, signalling pathways, and disease modules, making it particularly suited for the study of pleiotropic agents like Lanifibranor in complex diseases such as NAFLD (11). By combining databases such as GeneCards, STRING, and KEGG with bioinformatics tools, this approach can systematically reveal therapeutic mechanisms and potential off-target effects, thereby accelerating drug repurposing and precision medicine efforts.

In this study, we employed a network pharmacology approach to investigate the molecular mechanisms of Lanifibranor in the context of NAFLD. Our aim was to identify core targets, signalling pathways, and biological processes involved in Lanifibranor's therapeutic action, and to validate the compound's interaction potential using molecular docking simulations. This integrative strategy provides valuable insights into the systemic effects of Lanifibranor and supports its further development as a multitarget agent for NAFLD.

Materials and Methods

Collection of Drug Targets

The potential molecular targets of Lanifibranor were systematically retrieved on 20-07-2025 through comprehensive *in silico* screening using "PubChem (https://pubchem.ncbi.nlm.nih.gov) and SwissTargetPrediction (https://www.swisstargetprediction.ch)." The resulting protein targets were mapped to their corresponding gene symbols using "UniProt (https://www.uniprot.org)," on 20-07-2025 ensuring specificity to *Homo sapiens*. Redundant and non-human entries were excluded to curate a refined, high-confidence target dataset.

Collection of Disease-Associated Targets

To ensure a comprehensive identification of genes implicated in non-alcoholic fatty liver disease (NAFLD), gene datasets were systematically extracted from the "GeneCards (https://www.genecards.org)" on 22-07-2025. All retrieved targets were restricted to *Homo sapiens* and underwent rigorous deduplication to generate a refined, non-redundant list of disease-associated genes.

Network Construction

The intersection of Lanifibranor-associated targets with NAFLD-related genes was determined using "Venny 2.1.0 (https://bioinfogp.cnb.csic.es/tools/venny/)" on 22-07-2025 to identify potential therapeutic targets mediating drug–disease interactions. These overlapping targets were subsequently integrated into a Drug–Target–Disease (DTD) network, constructed and visualized using "Cytoscape v3.10.3 (https://cytoscape.org/)" on 24-07-2025. This network enabled a systems-level interpretation of molecular interactions, highlighting the key nodes potentially modulated by Lanifibranor in the context of NAFLD.

Construction of Protein–Protein Interaction (PPI) Network

To elucidate the molecular crosstalk among the putative therapeutic targets, a high-confidence PPI network was constructed using the STRING database (https://string-db.org) on 22-07-2025, restricting the organism to *Homo sapiens* and applying a stringent interaction confidence threshold of ≥0.7. The resultant interaction data were imported into Cytoscape v3.10.3 for network visualization and topological analysis. Core hub genes within the network were prioritized based on key centrality metrics—degree centrality, betweenness centrality, and closeness centrality—to identify potential molecular drivers of Lanifibranor's therapeutic action in NAFLD.

Vol. 20 (Supplementary Issue 2A), June 2026, ISSN 0973-8916 (Print)., 2230-7303 (Online)
10.5530/ctbp.2026.2s.14

Gene Ontology (GO) and KEGG Pathway Enrichment Analysis

To elucidate the biological relevance of the overlapping gene set, comprehensive functional enrichment analysis was performed using ShinyGO v0.82 (https://bioinformatics.sdstate.edu/go/) on 25-07-2025. Gene Ontology (GO) analysis was conducted to classify genes into Biological Processes (BP), Molecular Functions (MF), and Cellular Components (CC), while KEGG pathway analysis delineated the involvement of target genes in key metabolic and signalling pathways. An FDR-adjusted p-value cutoff of 0.05 was applied to ensure statistical robustness, and terms were prioritized based on both false discovery rate (FDR) and fold enrichment, highlighting functionally and biologically significant annotations.

Molecular Docking

Molecular docking was conducted using AutoDock Vina v1.1.2 (https://vina.scripps.edu) to evaluate the binding affinity of Lanifibranor with key NAFLD-associated protein targets. The 3D structures of selected proteins were retrieved from the RCSB Protein Data Bank (https://www.rcsb.org) and prepared using PyMOL (https://www.pymol.org) by retaining relevant chains and removing heteroatoms, co-crystallized ligands, and water molecules. Cleaned structures were saved in .pdb format and prepared in AutoDock Tools v1.5.7 (https://autodock.scripps.edu) by adding polar hydrogens, Kollman charges, and assigning AD4 atom types. Active binding pockets were predicted using PrankWeb (https://prankweb.cz), and grid boxes were defined around top-ranked pockets with the following center coordinates: 1GKC: (42.057, 16.192, 146.181), 3ERT: (−31.545, −0.876, 25.053), 4MAN: (−38.967, −22.835, −19.624), 5F1A: (45.005, 21.993, 238.493).

Ligands were retrieved from PubChem, energy-minimized, and converted into .pdbqt format. Docking simulations were executed using default Vina parameters, and binding affinities (in kcal/mol) were recorded. Complexes with the lowest binding energies were considered optimal. Docked poses were further analyzed and visualized using "Discovery Studio Visualizer (https://www.3ds.com/products/biovia/discovery-studio/visualization)" and "LigPlot+ v2.2 (https://www.ebi.ac.uk/thornton-srv/software/LigPlus/)" to identify key interaction residues and hydrogen bonding patterns.

Results and Discussion

Collection of Drug Targets

Potential therapeutic targets of Lanifibranor were systematically identified through integrative in silico screening using multiple publicly available databases. The PubChem database and the SwissTarget Prediction platform were utilized to predict and retrieve protein targets based on the compound's molecular structure and bioactivity profile. All retrieved targets were curated to retain only human-specific entries and de-duplicated to ensure dataset integrity. A total of 102 unique protein targets were identified. The complete list of these targets is presented in (Table 1).

NAFLD-Associated Target Genes

A comprehensive dataset comprising 1,526 genes associated with non-alcoholic fatty liver disease (NAFLD) was compiled through integrative data mining from authoritative sources, including GeneCards (https://www.genecards.org). These genes represent a wide spectrum of molecular targets implicated in the pathogenesis and progression of NAFLD, including metabolic dysfunction, inflammation, and fibrosis.

Network Construction

A total of 37 overlapping targets between Lanifibranor and NAFLD-associated genes were identified using Venny 2.1.0 (https://bioinfogp.cnb.csic.es/tools/venny/), indicating a significant intersection of therapeutic relevance shown in (Fig. 1). 37 intersecting targets between Lanifibranor and NAFLD-linked genes suggests a robust overlap with the disease's pathogenic machinery. These targets span metabolic regulators (PPARA, PPARG, PPARD), pro-

Vol. 20 (Supplementary Issue 2A), June 2026, ISSN 0973-8916 (Print)., 2230-7303 (Online)
10.5530/ctbp.2026.2s.14

Table 1: Predicted Targets of Lanifibranor Identified via In Silico Screening			
PPARA	PPARG	CCND1	PPARD
BCKDHA	PTGS1	PTGS2	AR
AKR1B1	CXCL8	AKR1C3	NOS2
BRD4	SLC22A12	FFAR1	EDNRA
ABCB1	MAPK14	CD38	GLO1
PTGER1	FNTA	FNTB	PFKFB3
ADAMTS5	TBXAS1	ACE	CCKAR
MME	BMP1	NTSR1	TOP1
MMP9	ITGAV	ITGB3	BAD
FDFT1	CTSA	TTR	CMA1
AKR1C4	PIK3CB	MMP2	KDM2B
KDM4C	ABAT	ITGB1	ITGA2
ALOX5	PYGL	LTB4R	CASP1
FABP1	PTGES	CPB1	RBP4
TACR3	MDM2	TRPM8	ITGA4
AGTR1	PTGER2	FABP4	FABP3
FABP5	PTGER3	MMP12	BCL2L1
BCL2	MMP13	MMP3	MMP1
CPT1A	PTGER4	AKR1A1	TGM2
MAPK1	MMP8	THRA	THRB
DAGLA	CA2	PDPK1	CA1
CA12	PTPN1	PTPRF	CA9
CSNK2A1	PTPN2	AKR1C2	CSF1R
PLA2G2A	ESR1	PIN1	ELANE
AKR1B10	KDM6B	SLC6A4	PLA2G2E
MAPK8	PLA2G5	PLA2G10	

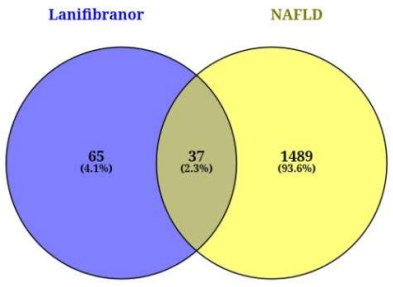

Fig. 1: Venn diagram showing the overlapping targets between Lanifibranor and NAFLD-associated targets. The overlapping region represents the common targets that may be modulated by Lanifibranor in NAFLD

inflammatory mediators (PTGS2, NOS2), oxidative stress markers (AKR1B1), matrix remodeling enzymes (MMP9, MMP2), and apoptosis regulators (BCL2)—underscoring Lanifibranor's systems-level mode of action (8). The pan-PPAR activation offers a unique advantage by modulating lipid metabolism (PPARα), insulin sensitivity (PPARγ), and inflammation/fibrosis (PPARδ), collectively addressing the multifaceted pathology of NAFLD (12).

A comprehensive Drug–Target–Disease interaction network was subsequently constructed and visualized using Cytoscape 3.10.3 (https://cytoscape.org/) as depicted in (Fig. 2). To identify key molecular targets, topological network analysis was performed based on degree centrality, betweenness centrality, and closeness centrality. Targets with the highest connectivity were identified as potential hub nodes, suggesting their critical involvement in modulating NAFLD-related pathogenic pathways. The interaction attributes and

Vol. 20 (Supplementary Issue 2A), June 2026, ISSN 0973-8916 (Print)., 2230-7303 (Online)
10.5530/ctbp.2026.2s.14

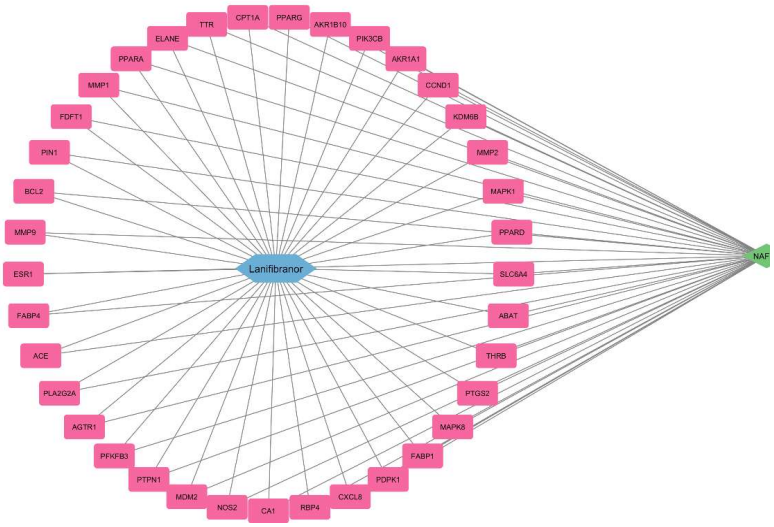

Fig. 2: Drug-target-disease network construction by Cytoscape. In this network, the green node represents NAFLD, pink nodes indicate the intersecting targets, and the blue node corresponds to Lanifibranor

Table 2: Topological analysis of network

Node name	Maximal Clique Centrality	Degree Centrality	Closeness Centrality	Betweenness Centrality
NAFLD	37	37	37.5	666
Lanifibranor	37	37	37.5	666
PPARA	2	2	20	0.05405
PPARG	2	2	20	0.05405
CCND1	2	2	20	0.05405
PPARD	2	2	20	0.05405
PTGS2	2	2	20	0.05405
CXCL8	2	2	20	0.05405
NOS2	2	2	20	0.05405
PFKFB3	2	2	20	0.05405
ACE	2	2	20	0.05405
MMP9	2	2	20	0.05405
ESR1	2	2	89.45	23.06414
BCL2	3	3	90.5	20.19675
MMP2	3	3	90.5	21.00137

topological parameters of these key targets are summarized in (Table 2).

Construction and Analysis of the Protein–Protein Interaction (PPI) Network

To elucidate the functional crosstalk among the 37 overlapped targets, a Protein–Protein Interaction (PPI) network was constructed using the STRING database (https://string-db.org/). The resulting network comprised 37 nodes, 58 edges, and an average node degree of 3.14, as illustrated in (Fig. 3). The PPI network was further analyzed in Cytoscape (v3.10.3), where

Vol. 20 (Supplementary Issue 2A), June 2026, ISSN 0973-8916 (Print)., 2230-7303 (Online)
10.5530/ctbp.2026.2s.14

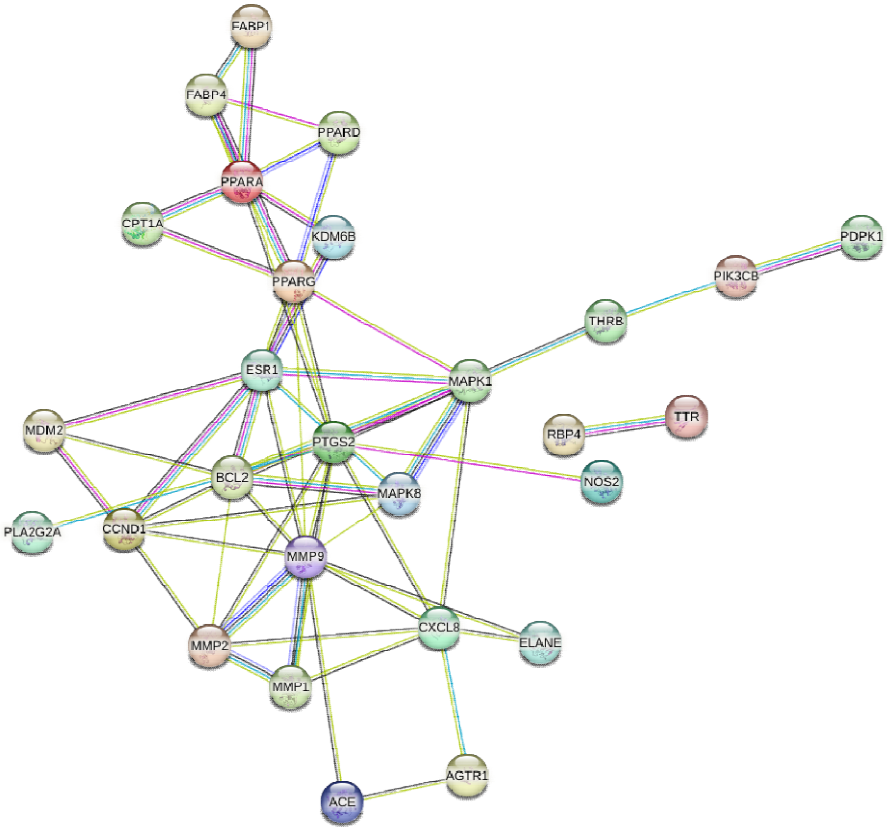

Fig. 3: Protein–protein interaction (PPI) network of overlapping targets between Lanifibranor and NAFLD, constructed using the STRING database. Nodes represent proteins, and edges represent predicted functional associations between them

topological analysis was performed using the CytoHubba plugin. Core hub genes were prioritized based on key network metrics—degree centrality, betweenness centrality, and closeness centrality. The top 10 hub genes identified by CytoHubba are shown in (Fig. 4), and their topological scores are detailed in (Table 3). Among these, the top five high-priority targets—MMP9, PTGS2, ESR1, BCL2, and MMP2—emerged as central regulatory nodes and in drug-target-disease network construction, notably, ESR1, BCL2, and MMP2 exhibited higher closeness and betweenness centrality than other targets, indicating greater regulatory influence and signal mediation potentially contributing to the mechanistic action of Lanifibranor in NAFLD. These targets were subsequently selected for molecular docking to assess their binding affinities and therapeutic potential.

Gene Ontology (GO) Enrichment Analysis

Gene Ontology enrichment analysis of the 37 overlapping targets revealed several significantly enriched biological processes (GO BP), indicating the functional roles of these genes in NAFLD pathology and their modulation by the compound under investigation. Among the enriched terms, as depicted in (Fig. 5a), “response to hypoxia” (GO:0001666) exhibited the highest fold enrichment (29.65) with 14 associated genes

Vol. 20 (Supplementary Issue 2A), June 2026, ISSN 0973-8916 (Print)., 2230-7303 (Online)
10.5530/ctbp.2026.2s.14

and a false discovery rate (FDR) of 9.51×10^{-15}. This suggests that hypoxia-driven signalling is a highly focused and overrepresented pathway among the common targets, underscoring the potential relevance of oxygen deprivation mechanisms in disease progression and therapeutic intervention. On the other hand, "response to oxygen-containing compound" (GO:1901700) emerged as the most statistically significant GO term, with an FDR of 2.75×10^{-19} and involving 27 genes. Despite a slightly lower fold enrichment (9.53), this process reflects the broader biological response to reactive oxygen species and other oxygenated molecules, which are critically involved in hepatic oxidative stress—a key driver of NAFLD pathophysiology, where impaired mitochondrial function and excess lipid accumulation promote reactive oxygen species (ROS) generation and tissue injury (13). These results highlight the dual role of the overlapping targets in both acute cellular responses to hypoxia and chronic oxidative stress adaptation, providing mechanistic insights into how the test compound may exert its hepatoprotective effects in NAFLD.

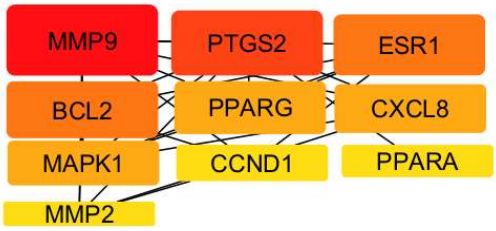

Fig. 4: Top 10 hub targets identified from the protein–protein interaction (PPI) network of overlapping Lanifibranor and NAFLD targets. The PPI data were imported into Cytoscape, and hub targets were ranked based on network topology parameters

Gene Ontology (GO) molecular function analysis displayed in (Fig. 5b), revealed that "long-chain fatty acid binding" (GO:0036041) had the highest fold enrichment (123.68) despite involving only 3 genes, indicating a highly specific yet critical functional role of these targets in lipid interaction relevant to NAFLD. In contrast, "enzyme binding" (GO:0019899) was identified as the most statistically significant term (FDR = 2.92×10^{-6}), involving 17 genes, suggesting a broader involvement of the targets in regulating catalytic processes that govern lipid metabolism and redox balance. These observations align with the pharmacological profile of Lanifibranor, a first-in-class pan-PPAR agonist that modulates all three PPAR isoforms (α, δ, and γ). PPARα activation enhances mitochondrial and peroxisomal β-oxidation of fatty acids, thereby reducing hepatic lipid overload (14). PPARδ contributes to improved insulin sensitivity and lipid utilization in peripheral tissues (15), while PPARγ supports adipose tissue lipid storage and attenuates hepatic stellate cell activation, a driver of fibrosis (16). Other enriched terms such as "nuclear receptor activity" and "zinc ion binding" also

Table 3: Topological scores of hub targets

Node name	MCC	MNC	Degree Centrality	EPC	Closeness Centrality	Betweenness Centrality
MMP9	67	10	11	12.343	17.11667	120.1695
PTGS2	41	7	10	12.072	17.08333	175.9652
ESR1	41	7	8	11.547	15.41667	63.45974
BCL2	50	8	8	11.95	15.25	35.00433
PPARG	11	4	7	10.623	15.41667	112.9333
MAPK1	15	6	7	11.29	15.5	151.0684
CXCL8	29	6	7	11.082	14.58333	64.80693
PPARA	7	3	6	8.373	13.78333	66.70952
CCND1	36	6	6	10.975	13.36667	7.21212
MMP2	36	6	6	11.279	13.95	8.59697

Vol. 20 (Supplementary Issue 2A), June 2026, ISSN 0973-8916 (Print)., 2230-7303 (Online)
10.5530/ctbp.2026.2s.14

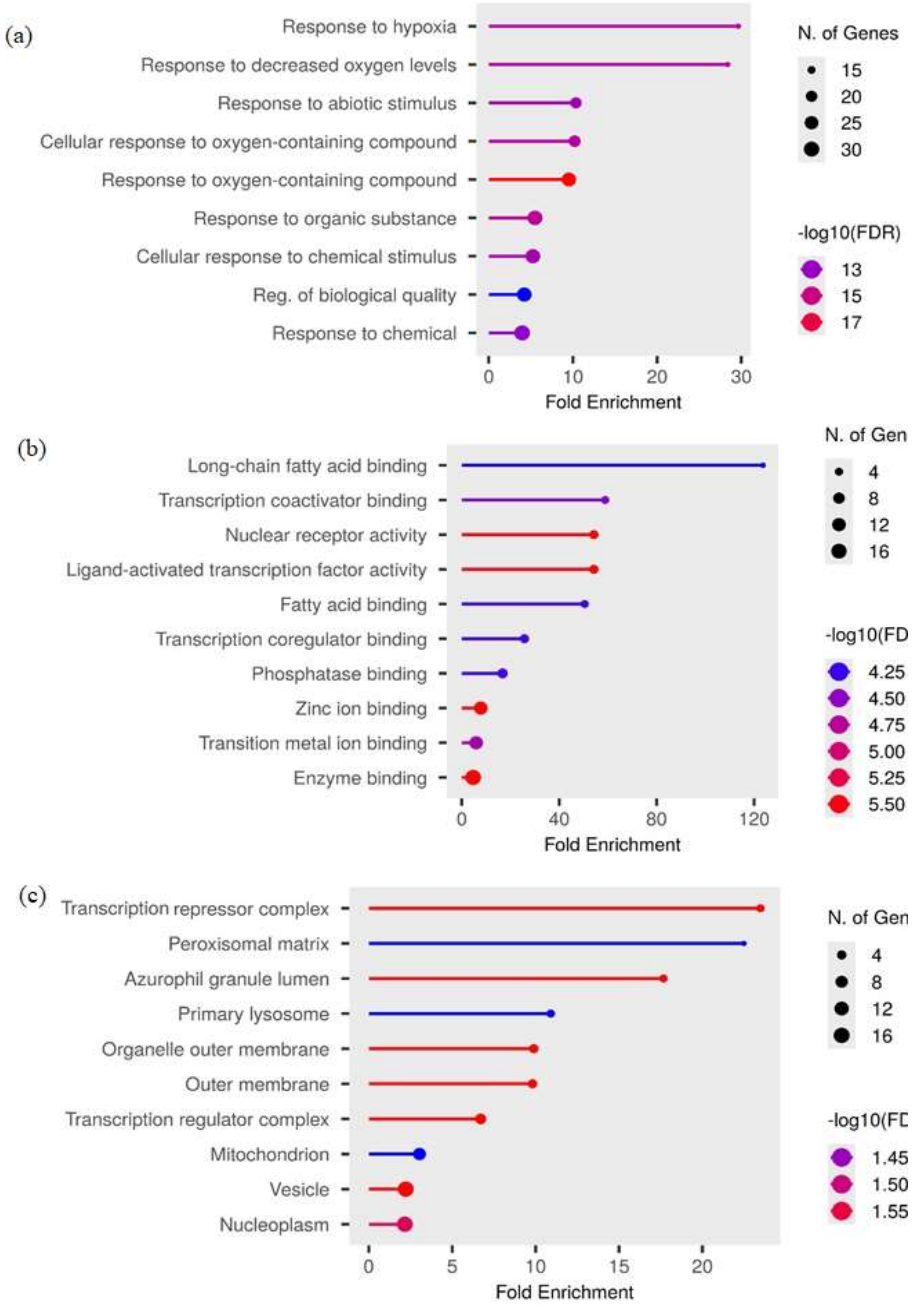

Fig. 5: Gene Ontology enrichment analysis of overlapped targets (a) Bar plot of Biological Process, (b) Bar plot of Molecular Function, (c) Bar plot of Cellular Component

Vol. 20 (Supplementary Issue 2A), June 2026, ISSN 0973-8916 (Print)., 2230-7303 (Online)
10.5530/ctbp.2026.2s.14

pointed toward key roles in transcriptional regulation and metal ion coordination, further emphasizing the molecular complexity of NAFLD pathophysiology.

From the GO cellular component enrichment analysis (Fig. 5c), the transcription repressor complex (GO:0017053) emerged as the most enriched term with a fold enrichment of 23.48 (FDR = 0.026), involving only three genes. This indicates a highly specific but critical localization, highlighting the importance of transcriptional repression in regulating gene expression associated with NAFLD progression. As nuclear receptors, PPARs interact directly with co-repressor and co-activator complexes to regulate lipid and glucose metabolism genes (17), thereby providing a direct mechanistic link between Lanifibranor's mode of action and the enrichment data. In contrast, the vesicle (GO:0031982) category included the largest number of genes (16 genes, fold enrichment = 2.21), suggesting a broader but biologically meaningful role in intracellular trafficking and secretion. Vesicle-associated processes are essential for lipid transport, cytokine release, and insulin signalling, all of which are central to NAFLD pathophysiology. Together, these findings underscore how NAFLD-related targets are distributed between highly specific nuclear regulatory sites and generalized cellular compartments.

KEGG Pathway Enrichment Analysis

KEGG pathway enrichment analysis revealed several significantly enriched pathways associated with NAFLD-related targets as shown in (Fig. 6a). Among them, the "Bladder cancer" pathway (hsa05219) showed the highest fold enrichment (105.58) with 7 genes out of 41 background genes, suggesting a strong overrepresentation despite the cancer-specific context, possibly reflecting shared oncogenic or metabolic signalling components. In contrast, the most statistically significant pathway was "Pathways in cancer" (hsa05200), involving 16 genes with an FDR of 9.34×10^{-15}, highlighting the systemic role of dysregulated signalling networks common to both NAFLD and oncogenic risk associated with chronic NASH, including transformation into hepatocellular carcinoma (HCC) (18). Other enriched pathways, such as PPAR signalling (hsa03320) and AGE-RAGE signalling in diabetic complications (hsa04933), further support the metabolic and inflammatory basis of NAFLD pathogenesis (Fig. 6b) (19). PPAR signalling pathway was obtained from KEGG database (https://www.genome.jp/kegg/pathway.html).

Molecular docking

Molecular docking done with hub targets to Lanifibranor, Reference drugs (Pioglitazone, Vitamin E, Obeticholic Acid, Doxycycline) and each target respective co-crystallized ligands. As shown in (Table 4), molecular docking revealed that Lanifibranor exhibited binding affinities ranging from –6.6 to –8.2 kcal/mol across five NAFLD-associated targets. It showed the strongest binding with PTGS2 (–8.2 kcal/mol) and BCL2 (–8.1 kcal/mol), suggesting anti-inflammatory (20) and anti-apoptotic potential (21). Moderate binding was observed with PPARG (–7.7 kcal/mol), ESR1 (–7.3 kcal/mol), and MMP9 (–6.6 kcal/mol). Among the reference drugs, Pioglitazone displayed the highest binding to MMP9 (–9.2 kcal/mol) and ESR1 (–8.4 kcal/mol) aligning with its known insulin-sensitizing and anti-fibrotic effects (22). Vitamin E showed strong interaction with ESR1 (–8.5 kcal/mol), while Obeticholic Acid showed good binding to ESR1 (-8.0 kcal/mol) and comparable affinity toward PTGS2 (–7.4 kcal/mol) and PPARG (–7.8 kcal/mol). Doxycycline exhibited consistent binding across all targets, especially PTGS2 (–7.5 kcal/mol) and ESR1 (–8.0 kcal/mol) and interactions of complexes are shown in (Fig. 7). Amino acid residues forming interactions with selected compounds displayed in (Table 5). Overall, Lanifibranor's binding affinities were more or less comparable to reference compounds and co-crystallized ligands, supporting its potential as

Vol. 20 (Supplementary Issue 2A), June 2026, ISSN 0973-8916 (Print)., 2230-7303 (Online)
10.5530/ctbp.2026.2s.14

Table 4: Molecular docking interactions (Binding affinity in kcal/mol)		
Targets	Compounds	(Binding affinity in kcal/mol)
MMP9 (PDB ID =1GKC)	Lanifibranor	-6.6
	Pioglitazone (Ref)	-9.2
	Vitamin E (Ref)	-6.2
	Obeticholic Acid (Ref)	-6.6
	Doxycycline (Ref)	-6.7
	NFH (Co-crystallized ligand)	-6.7
PTGS2 (PDB ID =5F1A)	Lanifibranor	-8.2
	Pioglitazone (Ref)	-8.3
	Vitamin E (Ref)	-8.1
	Obeticholic Acid (Ref)	-7.4
	Doxycycline (Ref)	-7.5
	PROTOPORPHYRIN IX CONTAINING CO (Co-crystallized ligand)	-7.6
ESR1 (PDB ID =3ERT)	Lanifibranor	-7.3
	Pioglitazone (Ref)	-8.4
	Vitamin E (Ref)	-8.5
	Obeticholic Acid (Ref)	-8.0
	Doxycycline (Ref)	-8.0
	4-HYDROXYTAMOXIFEN (Co-crystallized ligand)	-7.9
BCL2 (PDB ID =4MAN)	Lanifibranor	-8.1
	Pioglitazone (Ref)	-7.5
	Vitamin E (Ref)	-7.4
	Obeticholic Acid (Ref)	-7.4
	Doxycycline (Ref)	-7.3
	4-[4-({4'-chloro-3-[2-(dimethylamino) ethoxy]biphenyl-2-yl}methyl)piperazin-1-yl]-2-(1H-indol-5-yloxy)-N-({3-nitro-4-[(tetrahydro-2H-pyran-4-ylmethyl)amino]phenyl}sulfonyl)benzamide (Co-crystallized ligand)	-7.5
PPARG (PDB ID= 6ONJ)	Lanifibranor	-7.7
	Pioglitazone (Ref)	-8.3
	Vitamin E (Ref)	-7.8
	Obeticholic Acid (Ref)	-7.8
	Doxycycline (Ref)	-7.1
	2,4-THIAZOLIDIINEDIONE, 5-[[4-[2-(METHYL-2-PYRIDINYLAMINO) ETHOXY]PHENYL]METHYL]-(9CL) (Co-crystallized ligand)	-7.1

Vol. 20 (Supplementary Issue 2A), June 2026, ISSN 0973-8916 (Print)., 2230-7303 (Online)
10.5530/ctbp.2026.2s.14

(a)

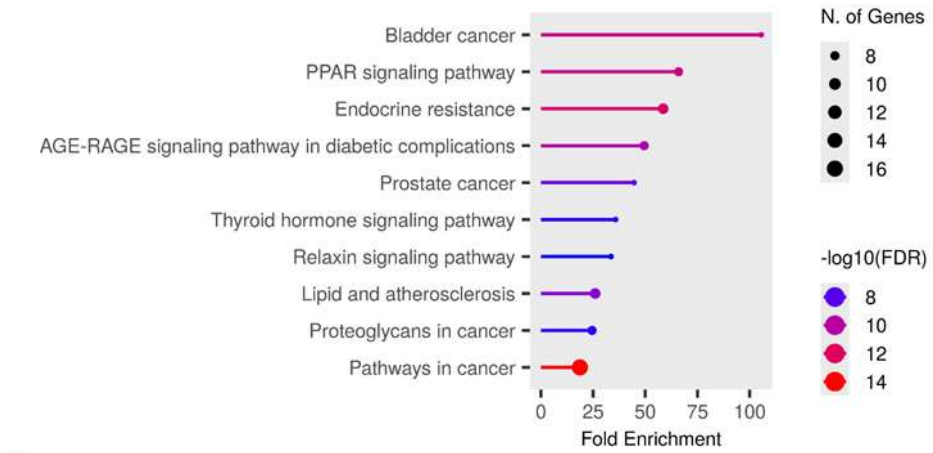

(b)

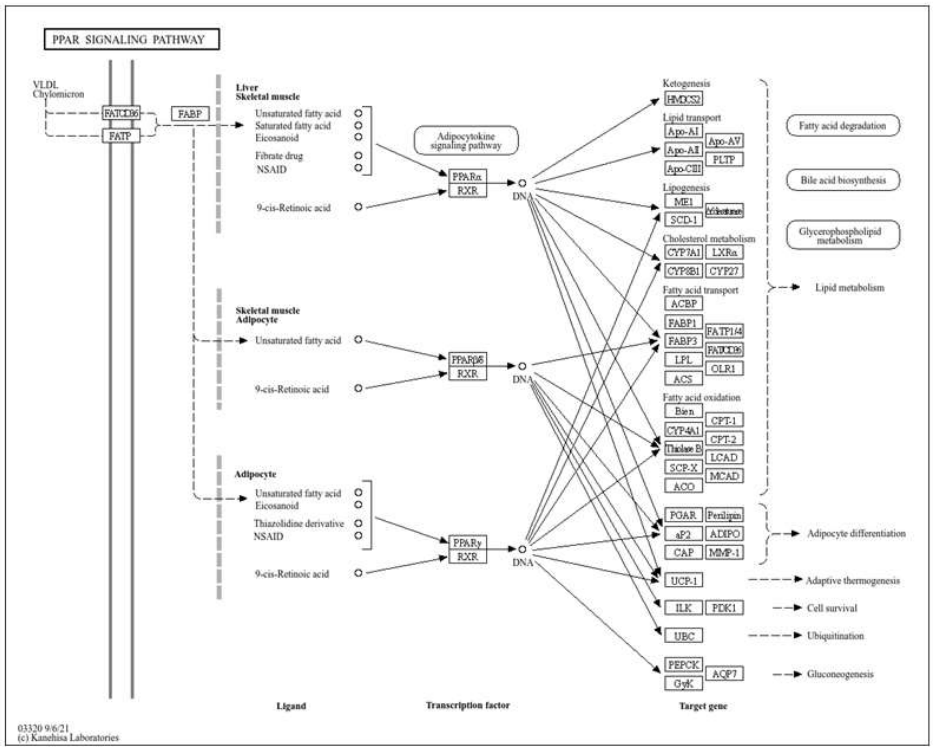

Fig. 6: KEGG Pathway Enrichment Analysis (a) Bar plot of KEGG, (b) PPAR signalling pathway obtained from KEGG database

Non-Alcoholic Fatty Liver Disease

Vol. 20 (Supplementary Issue 2A), June 2026, ISSN 0973-8916 (Print)., 2230-7303 (Online)
10.5530/ctbp.2026.2s.14

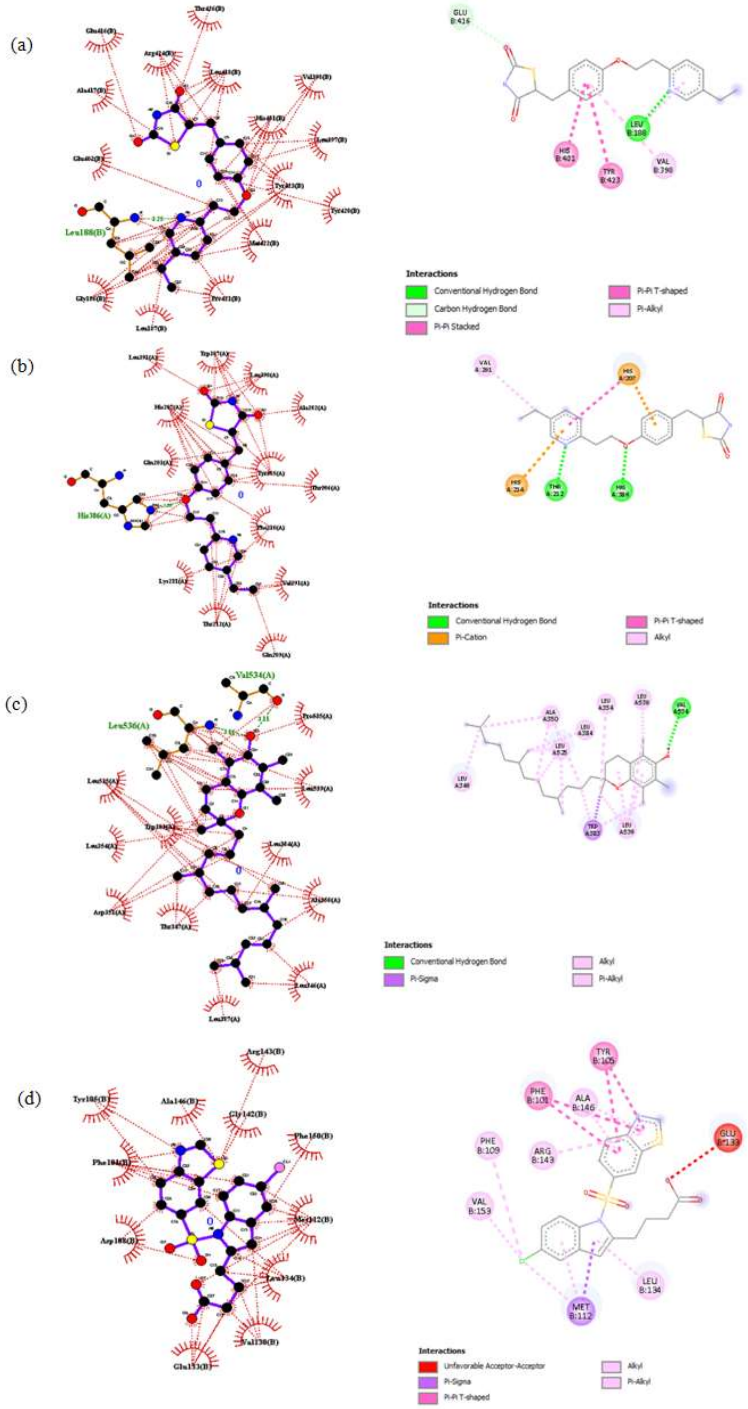

Vol. 20 (Supplementary Issue 2A), June 2026, ISSN 0973-8916 (Print)., 2230-7303 (Online)
10.5530/ctbp.2026.2s.14

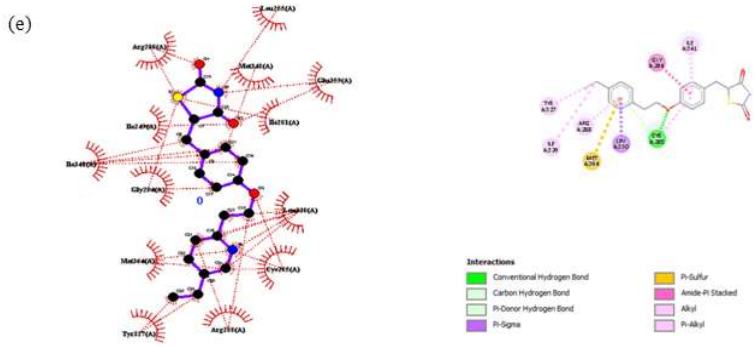

Fig. 7: Molecular docking interactions of (a) MMP9 **–** Pioglitazone, (b) PTGS2 -Pioglitazone, (c) ESR1 - Vitamin E, (d) BCL2 – Lanifibranor, (e) PPARG – Pioglitazone

Table 5: Amino acid residues involved in interactions with selected compounds

Target-complex	Residue name	Type of Interaction	Distance (Å)
MMP9 **–** Pioglitazone	LEU B:188	Hydrogen bond	3.25
	HIS B:401	Pi-Pi Stacked	4.62
	TYR B:423	Pi-Pi Stacked	5.18
PTGS2 -Pioglitazone	THR A:212	Hydrogen bond	2.19
	HIS A:386	Hydrogen bond	2.57
	HIS A:207	Pi- cation	3.33
ESR1 - Vitamin E	VAL A:534	Hydrogen bond	2.21
	TRP A:383	Pi-sigma	3.55
BCL2 – Lanifibranor	MET B:112	Pi-Sigma	3.77
	TYR B:105	Pi- Pi T shaped	4.83
PPARG – Pioglitazone	CYS A:285	Hydrogen bond	3.69
	LEU A:330	Pi-Sigma	3.88
	GLY A:284	Amide Pi-stacked	4.04

a multitarget agent. Although Lanifibranor did not surpass all references in binding strength, its comparable binding profile across diverse NAFLD targets supports its therapeutic versatility. These findings align with its pharmacological classification as a pan-PPAR agonist and highlight its capacity to influence multiple pathogenic pathways in NAFLD, including inflammation, lipid metabolism, apoptosis, and fibrosis (23). Recent reports support this observation, as Lanifibranor's binding affinities close to those of reference drugs strengthen its role as a promising pan-PPAR agonist with the ability to modulate multiple NAFLD-associated targets. Comparative simulations of the AF-2 domain of PPARs have provided mechanistic insights into how ligand-induced conformational changes stabilize co-activator recruitment, thereby enhancing transcriptional regulation of lipid and glucose metabolism (24). Similarly, high-throughput virtual screening, docking, and molecular dynamics studies of pharmacological ligands consistently highlight the therapeutic relevance of targeting lipid-sensing nuclear receptors with multi-target agonists, supporting the translational potential of Lanifibranor (25). In parallel, in silico and in vitro investigations on polydatin demonstrated pan-PPAR agonist activity, restoring hepatic lipid–energy balance and showing significant

Vol. 20 (Supplementary Issue 2A), June 2026, ISSN 0973-8916 (Print)., 2230-7303 (Online)
10.5530/ctbp.2026.2s.14

anti-NAFLD efficacy (26). Together, these findings underscore that Lanifibranor, in line with other validated pan-PPAR agonists, not only exhibits comparable binding strength to standard drugs but also embodies therapeutic versatility, making it a strong candidate for disease modification in NAFLD and related metabolic disorders.

Importantly, the overlap of NAFLD mechanisms with oncogenic and diabetic pathways implies that Lanifibranor may also serve as a disease-modifying agent with broader metabolic benefits, rather than merely addressing hepatic lipid accumulation.

We acknowledge that experimental validation is necessary to support these findings, even though the main foundation of this study is systems pharmacology and molecular docking techniques (27). In order to achieve this, we are starting in vitro tests to verify the target level and using refinement based on molecular dynamics to assess binding stability. Additionally, in vivo research in NAFLD models is being planned to evaluate the safety and effectiveness of the treatment. Furthermore, clinical studies of Lanifibranor in NASH patients (e.g., Phase II trial, NCT03008070) (8), have already shown histological improvement and a decrease in disease activity, which provides translational support for the therapeutic relevance of our findings. These validation efforts will be reported in future work and will provide crucial support for the translational potential of our computational predictions.

Conclusion

Our integrative analysis provides mechanistic insights into Lanifibranor's multi-target effects in NAFLD. We identified 37 overlapping targets between the drug and disease-associated genes, and network topological analysis highlighted hub proteins—MMP9, PTGS2, ESR1, BCL2, and PPARG—that regulate inflammation, apoptosis, fibrosis, and lipid metabolism. Gene Ontology and KEGG pathway enrichment analyses revealed key biological processes and pathways, including PPAR signalling, hypoxia response, and oxidative stress modulation. Molecular docking confirmed direct interactions with these hub targets, supporting the compound's multi-pathway therapeutic potential. Together, these findings provide a systems-level mechanistic framework that explains how Lanifibranor exerts its clinical benefits, extending beyond prior clinical observations. Further in vivo validation and clinical stratification are warranted to fully leverage its precision medicine potential in NAFLD.

Acknowledgement

We thank VFSTR deemed to be University for funding the study.

References

1. Younossi, Z.M., Koenig, A.B., Abdelatif, D., Fazel, Y., Henry, L., and Wymer, M. (2016). Global epidemiology of nonalcoholic fatty liver disease—meta-analytic assessment of prevalence, incidence, and outcomes. *Hepatology*, 64(1), 73–84.
2. Chalasani, N., Younossi, Z., Lavine, J.E., Charlton, M., Cusi, K., Rinella, M., Harrison, S.A., Brunt, E.M., and Sanyal, A.J. (2018). The diagnosis and management of nonalcoholic fatty liver disease: practice guidance from the American Association for the Study of Liver Diseases. *Hepatology*, 67(1), 328–357.
3. Estes, C., Razavi, H., Loomba, R., Younossi, Z., and Sanyal, A.J. (2018). Modeling the epidemic of nonalcoholic fatty liver disease demonstrates an exponential increase in burden of disease. *Hepatology*, 67(1), 123–133.
4. Buzzetti, E., Pinzani, M., and Tsochatzis, E.A. (2016). The multiple-hit pathogenesis of non-alcoholic fatty liver disease (NAFLD). *Metabolism*, 65(8), 1038–1048.
5. Nielsen, M.H., Nøhr-Meldgaard, J., Møllerhøj, M.B., Oró, D., Pors, S.E., Andersen, M.W., Kamzolas, I., Petsalaki, E., Vacca, M., Harder, L.M., and Perfield, J.W. (2025). Characterization of six clinical drugs

Vol. 20 (Supplementary Issue 2A), June 2026, ISSN 0973-8916 (Print)., 2230-7303 (Online)
10.5530/ctbp.2026.2s.14

and dietary intervention in the nonobese CDAA-HFD mouse model of MASH and progressive fibrosis. *American Journal of Physiology-Gastrointestinal and Liver Physiology*, 328(1), G51–G71.

6. Rolver, M.G., Severin, M., and Pedersen, S.F. (2024). Regulation of cancer cell lipid metabolism and oxidative phosphorylation by microenvironmental acidosis. *American Journal of Physiology-Cell Physiology*, 327(4), C869–C883.

7. Cooreman, M.P., Butler, J., Giugliano, R.P., Zannad, F., Dzen, L., Huot-Marchand, P., Baudin, M., Beard, D.R., Junien, J.L., Broqua, P., and Abdelmalek, M.F. (2024). The pan-PPAR agonist lanifibranor improves cardiometabolic health in patients with metabolic dysfunction-associated steatohepatitis. *Nature Communications*, 15(1), 3962.

8. Francque, S.M., Bedossa, P., Ratziu, V., Anstee, Q.M., Bugianesi, E., Sanyal, A.J., Loomba, R., Harrison, S.A., Balabanska, R., Mateva, L., Lanthier, N., Alkhouri, N., Moreno, C., Schattenberg, J.M., Stefanova-Petrova, D., Vonghia, L., Rouzier, R., Guillaume, M., Hodge, A., Romero-Gómez, M., Huot-Marchand, P., Baudin, M., Richard, M.P., Abitbol, J.L., Broqua, P., Junien, J.L., and Abdelmalek, M.F. (2021). A randomized, controlled trial of the pan-PPAR agonist lanifibranor in NASH. *New England Journal of Medicine*, 385(17), 1547–1558.

9. Barb, D., Kalavalapalli, S., Leiva, E.G., Bril, F., Huot-Marchand, P., Dzen, L., Rosenberg, J.T., Junien, J.L., Broqua, P., Rocha, A.O., Lomonaco, R., Abitbol, J.L., Cooreman, M.P., and Cusi, K. (2025). Pan-PPAR agonist lanifibranor improves insulin resistance and hepatic steatosis in patients with T2D and MASLD. *Journal of Hepatology*.

10. Hopkins, A.L. (2008). Network pharmacology: the next paradigm in drug discovery. *Nature Chemical Biology*, 4(11), 682–690.

11. Zhou, W., Wang, Y., Lu, A., and Zhang, G. (2016). Systems pharmacology in small molecular drug discovery. *International Journal of Molecular Sciences*, 17(2), 246.

12. Tailleux, A., Wouters, K., and Staels, B. (2012). Roles of PPARs in NAFLD: potential therapeutic targets. *Biochimica et Biophysica Acta (BBA)-Molecular and Cell Biology of Lipids*, 1821(5), 809–818.

13. Friedman, S.L., Neuschwander-Tetri, B.A., Rinella, M., and Sanyal, A.J. (2018). Mechanisms of NAFLD development and therapeutic strategies. *Nature Medicine*, 24(7), 908–922.

14. Pawlak, M., Lefebvre, P., and Staels, B. (2015). Molecular mechanism of PPARα action and its impact on lipid metabolism, inflammation and fibrosis in non-alcoholic fatty liver disease. *Journal of Hepatology*, 62(3), 720–733.

15. Barish, G.D., Narkar, V.A., and Evans, R.M. (2006). PPARδ: a dagger in the heart of the metabolic syndrome. *The Journal of Clinical Investigation*, 116(3), 590–597.

16. Miyahara, T., Schrum, L., Rippe, R., Xiong, S., Yee, H.F., Motomura, K., Anania, F.A., Willson, T.M., and Tsukamoto, H. (2000). Peroxisome proliferator-activated receptors and hepatic stellate cell activation. *Journal of Biological Chemistry*, 275(46), 35715–35722.

17. Chandra, V., Huang, P., Hamuro, Y., Raghuram, S., Wang, Y., Burris, T.P., and Rastinejad, F. (2008). Structure of the intact PPAR-γ–RXR-α nuclear receptor complex on DNA. *Nature*, 456(7220), 350–356.

18. Baffy, G. (2013). Hepatocellular carcinoma in non-alcoholic fatty liver disease: epidemiology, pathogenesis, and prevention. *Journal of Clinical and Translational Hepatology*, 1(2), 131–138.

19. Buckley, S.T., and Ehrhardt, C. (2010). The receptor for advanced glycation end products (RAGE) and the lung. *BioMed Research International*, 2010, 917108.

20. Simon, L.S. (1999). Role and regulation of cyclooxygenase-2 during inflammation. *The American Journal of Medicine*, 106(5), 37S–42S.

21. Malhi, H., and Gores, G.J. (2008). Cellular and molecular mechanisms of liver injury. *Gastroenterology*, 134(6), 1641–1654.

Vol. 20 (Supplementary Issue 2A), June 2026, ISSN 0973-8916 (Print)., 2230-7303 (Online)
10.5530/ctbp.2026.2s.14

22. Lonardo, A., Nascimbeni, F., Ballestri, S., Fairweather, D., Win, S., Than, T.A., Abdelmalek, M.F., and Suzuki, A. (2019). Sex differences in nonalcoholic fatty liver disease: state of the art and identification of research gaps. *Hepatology*, 70(4), 1457–1469.
23. Mantovani, A., Byrne, C.D., and Targher, G. (2022). Efficacy of peroxisome proliferator-activated receptor agonists, glucagon-like peptide-1 receptor agonists, or sodium-glucose cotransporter-2 inhibitors for treatment of non-alcoholic fatty liver disease: a systematic review. *The Lancet Gastroenterology & Hepatology*, 7(4), 367–378.
24. Gul, F., Parvaiz, N., and Azam, S.S. (2023). Deciphering the relational dynamics of AF-2 domain of PAN PPAR through drug repurposing and comparative simulations. *PLoS One*, 18(3), e0283743.
25. Mandal, S.K., Puri, S., Kumar, B.K., Muzaffar-Ur-Rehman, M., Sharma, P.K., Sankaranarayanan, M., and Deepa, P.R. (2024). Targeting lipid-sensing nuclear receptors PPAR (α, γ, β/δ): HTVS and molecular docking/dynamics analysis of pharmacological ligands as potential pan-PPAR agonists. *Molecular Diversity*, 28(3), 1423–1438.
26. Mandal, S.K., Muzaffar-Ur-Rehman, M., Puri, S., Sharma, P.K., Murugesan, S., and Deepa, P.R. (2025). In silico and in vitro investigations reveal pan-PPAR agonist activity and anti-NAFLD efficacy of polydatin by modulating hepatic lipid-energy metabolism. *Scientific Reports*, 15(1), 26995.
27. Ekins, S., Mestres, J., and Testa, B. (2007). In silico pharmacology for drug discovery: methods for virtual ligand screening and profiling. *British Journal of Pharmacology*, 152(1), 9–20.